Algorithms for the electronic and vibrational properties of nanocrystals

2009 J. Phys.: Condens. Matter 21 064207

(http://iopscience.iop.org/0953-8984/21/6/064207)

J. Phys.: Condens. Matter **21** (2009) 064207 (7pp) doi:10.1088/0953-8984/21/6/064207

Algorithms for the electronic and vibrational properties of nanocrystals

James R Chelikowsky[1,2,3], Alexey T Zayak[1], T-L Chan[1], Murilo L Tiago[4], Yunkai Zhou[5] and Yousef Saad[6]

[1] Center for Computational Materials, Institute for Computational Engineering and Sciences, University of Texas, Austin, TX 78712, USA
[2] Department of Physics, University of Texas, Austin, TX 78712, USA
[3] Department of Chemical Engineering, University of Texas, Austin, TX 78712, USA
[4] Materials Science and Technology Division, Oak Ridge National Laboratory, Oak Ridge, TN 37831, USA
[5] Department of Mathematics, Southern Methodist University, Dallas, TX 75275, USA
[6] Department of Computer Science and Engineering, University of Minnesota, Minneapolis, MN 55455, USA

E-mail: jrc@ices.utexas.edu

Received 27 June 2008, in final form 9 July 2008
Published 20 January 2009
Online at stacks.iop.org/JPhysCM/21/064207

Abstract
Solving the electronic structure problem for nanoscale systems remains a computationally challenging problem. The numerous degrees of freedom, both electronic and nuclear, make the problem impossible to solve without some effective approximations. Here we illustrate some advances in algorithm developments to solve the Kohn–Sham eigenvalue problem, i.e. we solve the electronic structure problem within density functional theory using pseudopotentials expressed in real space. Our algorithms are based on a nonlinear Chebyshev filtered subspace iteration method, which avoids computing explicit eigenvectors except at the first self-consistent-field iteration. Our method may be viewed as an approach to solve the original nonlinear Kohn–Sham equation by a nonlinear subspace iteration technique, without emphasizing the intermediate linearized Kohn–Sham eigenvalue problems. Replacing the standard iterative diagonalization at each self-consistent-field iteration by a Chebyshev subspace filtering step results in a significant speed-up, often an order of magnitude or more, over methods based on standard diagonalization. We illustrate this method by predicting the electronic and vibrational states for silicon nanocrystals.

(Some figures in this article are in colour only in the electronic version)

1. Introduction

One of the most significant goals in computational physics is the development of new algorithms and physical concepts for describing matter at all length scales, especially at the nanoscale. This goal has assumed more significance owing to interest in the role of quantum size effects or quantum confinement [1]. Quantum confinement offers one the opportunity to alter the physical properties of matter without changing the chemical composition. For example, quantum confinement in CdSe nanocrystals can be used to tune the optical gap across the visible spectrum [2]. Also, Si crystals can be made optically active at nanolength scales [3, 4].

Achieving an efficacious algorithm for predicting the role of quantum confinement and its role in determining the properties of nanocrystals is a difficult task owing to the complexity of nanocrystals, which often contain thousands of atoms. However, notable progress has been accomplished by implementing new algorithms designed for highly parallel platforms.

2. The electronic structure problem

The spatial and energetic distributions of electrons can be described by a solution of the Kohn–Sham equation [5]:

$$\left(\frac{-\hbar^2\nabla^2}{2m} + V_{\text{ion}}^{\text{p}} + V_{\text{H}} + V_{\text{xc}}\right)\psi_n = E_n\psi_n \qquad (1)$$

where $V_{\text{ion}}^{\text{p}}$ is an ionic pseudopotential [6, 7], V_{H} is the Hartree or Coulomb potential and V_{xc} is the exchange–correlation potential. The Hartree and exchange–correlation potentials can be determined from the electronic charge density. The density is given by

$$\rho(\vec{r}) = e \sum_{n,\text{occup}} |\psi_n(\vec{r})|^2. \tag{2}$$

The summation is over all occupied states. The Hartree potential is then determined by

$$\nabla^2 V_{\text{H}}(\vec{r}) = -4\pi e \rho(\vec{r}). \tag{3}$$

This term can be interpreted as the electrostatic interaction of an electron with the charge density of the system.

The exchange–correlation potential is more problematic. This potential can be evaluated using a *local density approximation*. The central tenet of this approximation is that the total exchange–correlation energy may be written as a universal functional of the density:

$$E_{\text{xc}}[\rho] = \int \rho(\vec{r}) \epsilon_{\text{xc}}[\rho(\vec{r})] \, \mathrm{d}^3 r, \tag{4}$$

where ϵ_{xc} is the exchange–correlation energy density. E_{xc} and ϵ_{xc} are to be interpreted as depending solely on the charge density. The exchange–correlation potential, V_{xc}, is then obtained as $V_{\text{xc}} = \delta E_{\text{xc}}[\rho]/\delta\rho$.

It is not difficult to solve the Kohn–Sham equation (equation (1)) for an atom. This atomic solution provides the input to construct a pseudopotential representing the effect of the core electrons and nucleus. This 'ion core' pseudopotential, $V_{\text{ion}}^{\text{p}}$, can be transferred to other systems such as molecules and nanocrystals [6, 7].

The Kohn–Sham equations represent a nonlinear, self-consistent eigenvalue problem. Typically, a solution is obtained by first approximating the Hartree and exchange–correlation potentials using a superposition of atomic charge densities. The Kohn–Sham equation is then solved using these approximate potentials. From the solution, new wavefunctions and charge densities are obtained and used to construct updated Hartree and exchange–correlation potentials. The process is repeated until the 'input' and 'output' potentials agree and a self-consistent solution is realized. At this point, the total electronic energy can be computed along with a variety of other electronic properties [6, 7].

Once the Kohn–Sham equation is solved, the total electronic energy, E_{T}, of the system can be evaluated from

$$E_{\text{T}} = \sum_{n,\text{occup}} E_n - \tfrac{1}{2} \int V_{\text{H}}(\vec{r}) \rho(\vec{r}) \, \mathrm{d}^3 r + \int \rho(\vec{r}) (\epsilon_{\text{xc}}[\rho(\vec{r})] - V_{\text{xc}}[\rho(\vec{r})]) \, \mathrm{d}^3 r. \tag{5}$$

The structural energy can be obtained by adding the ion core electrostatic terms [6, 7]. Interatomic forces can be obtained by taking the derivative of the energy with respect to position.

3. Algorithms for solving the Kohn–Sham equation

The Kohn–Sham equation as cast in equation (1) can be solved using a variety of techniques. Often the wavefunctions can be expanded in a basis such as plane waves or Gaussians and the resulting secular equations can be solved using standard diagonalization packages such as those found in VASP [8].

Here we focus on a different approach. We solve the Kohn–Sham equation without resort to an explicit basis [9–13]. We solve for the wavefunctions on a uniform grid within a fixed domain. The wavefunctions outside of the domain are required to vanish for confined systems or assume periodic boundary conditions for systems with translational symmetry. In contrast to methods employing an explicit basis, such boundary conditions are easily incorporated. In particular, real space methods do not require the use of supercells for localized systems. As such, charged systems can easily be examined without considering any electrostatic divergences.

Within a 'real space' approach, one can solve the eigenvalue problem using a finite element or finite difference approach [10, 11, 13]. We use a higher-order finite difference approach owing to its simplicity in implementation. The Laplacian operator can be expressed using

$$\left(\frac{\partial^2 \psi}{\partial x^2}\right)_{x_0} \approx \sum_{n=-N}^{N} A_n \, \psi(x_0 + nh, y, z), \tag{6}$$

where h is the grid spacing, N is the number of nearest grid points and A_n are the coefficients for evaluating the required derivatives [14]. The error scales as $O(h^{2N+2})$.

Once the secular equation is created, the eigenvalue problem can be solved using iterative methods [12, 15, 16]. Typically, a method such as a preconditioned Davidson method can be used [12]. This is a robust and efficient method, which never requires one to store the Hamiltonian matrix. Our method utilizes a damped *Chebyshev polynomial filtered subspace iteration*. In our approach, only the initial iteration necessitates solving an eigenvalue problem, which can be handled by means of any available efficient eigensolver. This step is used to provide a good initial subspace (or good initial approximation to the wavefunctions). Because the subspace dimension is slightly larger than the number of wanted eigenvalues, the method does not utilize as much memory as standard restarted eigensolvers such as ARPACK and TRLan (Thick–Restart, Lanczos) [17, 18]. Moreover, the cost of orthogonalization is much reduced as the filtering approach only requires a subspace with dimension slightly larger than the number of occupied states and orthogonalization is performed only once per SCF iteration. In contrast, standard eigensolvers using restart usually require a subspace at least twice as large and the orthogonalization and other costs related to updating the eigenvectors are much higher.

The main idea of the proposed method is to start with a good initial eigenbasis, $\{\psi_n\}$, corresponding to occupied states of the initial Hamiltonian, and then to improve adaptively the subspace by polynomial filtering. That is, at a given self-consistent step, a polynomial filter, $P_m(t)$, of order m is constructed for the current Hamiltonian $\mathcal{H}$. As the eigenbasis

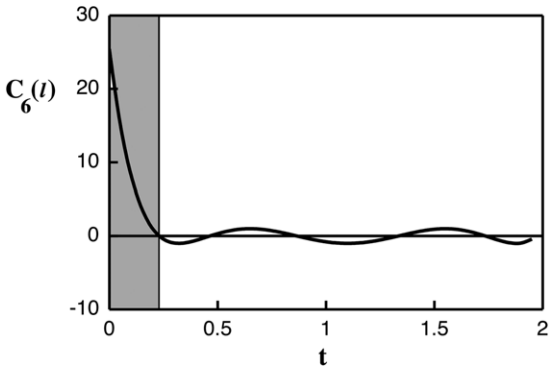

Figure 1. Schematic example of a damped Chebyshev polynomial, C_6. The shaded area corresponds to a hypothetical eigenvalue spectrum regime that will be enhanced by the filtering operation (see the text).

is updated, the polynomial will be different at each SCF step since $\mathcal{H}$ will change. The goal of the filter is to make the subspace spanned by $\{\hat{\psi}_n\} = P_m(\mathcal{H})\{\psi_n\}$ approximate the eigensubspace corresponding to the occupied states of $\mathcal{H}$. There is no need to make the new subspace, $\{\hat{\psi}_n\}$, approximate the wanted eigensubspace of $\mathcal{H}$ to high accuracy at intermediate steps. Instead, the filtering is designed so that the new subspace obtained at each self-consistent iteration step will progressively approximate the wanted eigenspace of the final Hamiltonian when self-consistency is reached.

This can be efficiently achieved by exploiting the Chebyshev polynomials, C_m, for the polynomials P_m. Specifically, we wish to exploit the dramatic increase in magnitude of the polynomial outside of the $[-1, 1]$ interval. All that is required to obtain a good filter at a given SCF step is to provide a lower bound and an upper bound of an interval of the spectrum of the current Hamiltonian $\mathcal{H}$. The lower bound can be readily obtained from the Ritz values computed from the previous step, and the upper bound can be inexpensively obtained by a very small number (e.g. four or five) of Lanczos steps [12]. Hence the main cost of the filtering at each iteration is in performing the products of the polynomial of the Hamiltonian by the basis vectors.

To construct a 'damped' Chebyshev polynomial on the interval $[a, b]$ to the interval $[-1,1]$, one can use an affine mapping such that

$$l(t) = \frac{t - (a+b)/2}{(b-a)/2}. \tag{7}$$

The interval is chosen to encompass the energy interval containing the eigenspace to be filtered, i.e. the lowest to highest eigenvalues. The filtering operation can then be expressed as

$$\{\hat{\psi}_n\} = C_m(l(\mathcal{H}))\{\psi_n\}. \tag{8}$$

This computation is accomplished by exploiting the convenient three-term recurrence property of Chebyshev polynomials:

$$\begin{aligned} C_0(t) &= 1, \qquad C_1(t) = t, \\ C_{m+1}(t) &= 2tC_m(t) - C_{m-1}(t). \end{aligned} \tag{9}$$

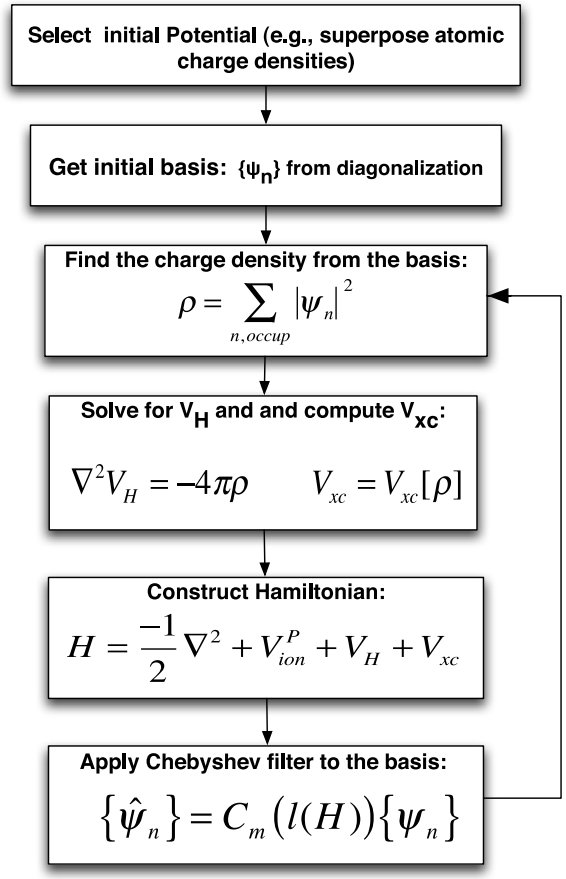

Figure 2. Schematic of the self-consistent cycle using Chebyshev filtering.

An example of a damped Chebyshev polynomial as defined by equations (7) and (9) is given in figure 1 where we have taken the lower bound as $a = 0.2$ and the upper bound as $b = 2$. In this example, the filtering would enhance the eigenvalue components in the shaded region.

The filtering procedure for the self-consistent cycle is illustrated in figure 2. Unlike traditional methods, the cycle only requires one explicit diagonalization step. Instead of repeating this step again within the self-consistent loop, a filtering operation is used to create a new basis in which the desired eigensubspace is enhanced. After the new basis, $\{\hat{\psi}_n\}$, is formed, the basis is orthogonalized. The orthogonalization step scales as the cube of the number of occupied states and, as such, this method is not an 'order-n' method. However, the prefactor is sufficiently small that the method is much faster than previous implementations of real space methods [12]. The cycle is repeated until the 'input' and 'output' density is unchanged.

The performance of our code on parallel computers follows the typical scaling behavior of parallel applications. Figure 3 shows the speed-up as a function of the total number of processors. Performance tests were done on Franklin, a Cray XT4 system maintained by NERSC. The saturation at the high-end side is caused by two factors: portions of the code are not parallelized (the crucial portions are well parallelized, but some initialization functions are executed

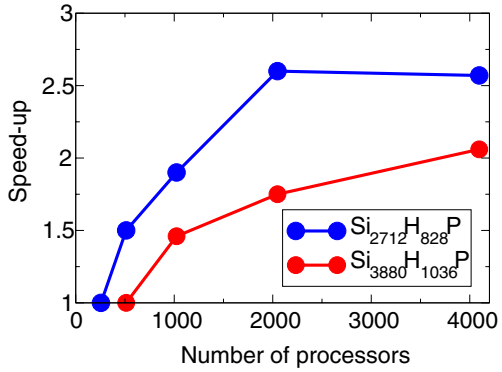

Figure 3. Examples of performance scaling for the real space pseudopotential code.

Table 1. Comparison of computational timings for various methods for a nanocrystal: $Si_{525}H_{276}$. While the number of SCF iterations is comparable for all three methods, the total time with filtering methods can be dramatically reduced.

Method	SCF Its	CPU(s)
Filtering	11	5947
ARPACK	10	62026
TRLan	10	26853

by a master processor only); and increasing the number of processors but keeping the same problem size increases the amount of data transferred among processors. The speed-up is inversely proportional to the total run time. With fixed problem size, the run time is the sum of time spent on distributed operations T_p and time spent on nondistributed operations T_0: $S = \text{const}/(T_0 + \frac{T_p}{N_p})$, where N_p is the number of processors. The equation is Amdahl's law of parallel speed-up [19]. The ratio of constants T_p/T_0 is an estimate of the maximum number of processors below which parallel scaling is preserved. In the example of figure 3, the ratio is 520 and 700, respectively, for $Si_{2712}H_{828}P$ and $Si_{3880}H_{1036}P$, thus showing good scaling up to approximately 512–1000 processors. Larger problem sizes have higher turning points, so that scaling improves with system size.

In table 1, we compare the timings using the Chebyshev filtering method along with explicit diagonalization solvers using the TRLan and ARPACK. These timing are for a modest sized nanocrystal: $Si_{525}H_{276}$. The Hamiltonian size is $292\,584 \times 292\,584$ and 1194 eigenvalues were determined. The numerical runs were performed on the SGI Altix 3700 cluster at the Minnesota Supercomputing Institute. The CPU type is a 1.3 GHz Intel Madison processor. Although the number of matrix-vector products and SCF iterations is similar, the total time with filtering is over an order of magnitude faster compared to ARPACK and a factor of better than four versus the TRLan. Such improved timings are not limited to this particular example.

4. Electronic properties of silicon nanocrystals

We illustrate the Chebyshev filtering method for a nanoscale system: hydrogenated silicon nanocrystals [12]. The systems

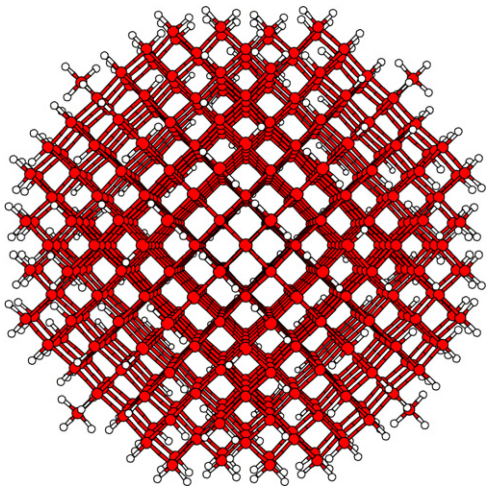

Figure 4. A ball and stick model of a hydrogenated silicon quantum dot. The interior consists of a diamond fragment. The surface of the fragment is capped with hydrogen atoms.

considered here are beyond the computational limits of 'standard' methods for obtaining a solution to the Kohn–Sham problem.

Nanocrystals are small fragments of the bulk in which the surface has been passivated; passivated nanocrystals correspond to 'quantum dots'. In the case of silicon, the passivation is accomplished experimentally by capping the surface dangling bonds with hydrogen atoms [20]. These systems exhibit interesting changes as one approaches the nanoregime [20, 21]. The largest nanocrystal we examined contained over ten thousand atoms: $Si_{9041}H_{1860}$, which is approximately 7 nm in diameter [12] as illustrated in figure 4.

We can also examine the evolution of the ionization potentials (I) and the electron affinities (A) for the quantum dot:

$$\begin{aligned} I &= E(N-1) - E(N) \\ A &= E(N) - E(N+1). \end{aligned} \tag{10}$$

The difference between the ionization potential and the electron affinity can be associated with the quasi-particle gap: $E_{qp} = I - A$. If the exciton (electron–hole) interaction is small, this gap can be compared to the optical gap. However, for silicon nanocrystals the exciton energy is believed to be of the order of $\sim$1 eV for nanocrystals of less than $\sim$1 nm.

We can examine the scaling of the ionization potential and affinity by assuming a simple scaling and fitting to the calculated values (shown in figure 5):

$$\begin{aligned} I(D) &= I_\infty + A/D^\alpha \\ A(D) &= A_\infty + B/D^\beta \end{aligned} \tag{11}$$

where D is the dot diameter. A fit of these quantities results in $I_\infty = 4.5$ eV, $A_\infty = 3.9$ eV, $\alpha = 1.1$ and $\beta = 1.08$. The fit gives a quasi-particle gap of $E_{qp}(D \to \infty) = I_\infty - A_\infty = 0.6$ eV in the limit of an infinitely large dot. This value is in good agreement with the gap found for crystalline silicon using the local density approximation [22]. The gap is not in good agreement with experiment owing to the failure of

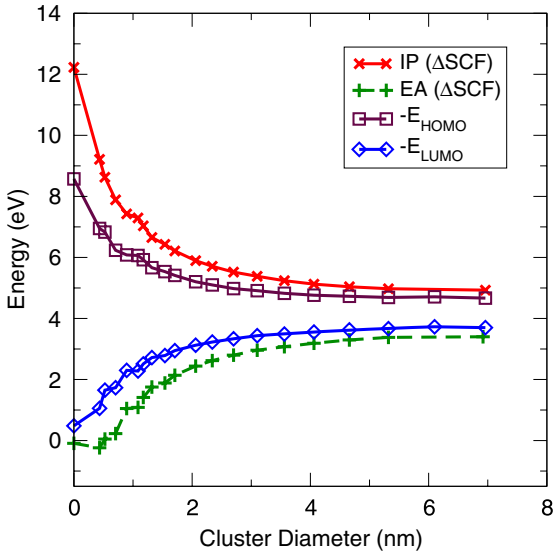

Figure 5. Evolution of the ionization potential (IP) and electron affinity (EA) with quantum dot size. Also shown are the eigenvalue levels for the highest occupied molecular orbital (HOMO) and the lowest unoccupied molecular orbital (LUMO).

the local density approximation to describe bandgaps of bulk semiconductors in general.

A key aspect of our study is that we can examine the scaling of the ionization potential and electron affinity for nanocrystals ranging from silane (SiH_4) to systems containing thousands of atoms. We not only verify the limiting value of the quasi-particle gap, we can ascertain how this limit is reached, i.e. how the ionization potential and electron affinity scale with the size of the dot and what the relationship is between these quantities and the highest occupied and lowest empty energy levels. At small sizes, the quasi-particle gap will likely be correct as the ionization potential and electron affinity are accurately determined by density functional theory for atoms and molecules. As the dot grows, we expect errors to be introduced, but the details are problematic without comparisons to experimental data.

5. Vibrational modes for silicon nanocrystals

Given the energy as a function of position, we can also examine structural and vibrational properties of nanocrystals. Vibrational properties are easier to describe as they converge more rapidly to the bulk values than do electronic states; however, because they involve small changes in energy with position, the wavefunctions need to be more highly converged.

Owing to the localized nature of nanocrystals, it is feasible to predict vibrational mode calculations by the direct force-constant method [23]. The dynamical matrix of the system is constructed by displacing all atoms one by one from their equilibrium positions along the Cartesian directions and finding the forces induced on the other atoms of the nanocrystal. We determine the forces using the Hellmann–Feynman theorem in real space [24] and employed a symmetrized form of the dynamical matrix expression [25]. The elements of the dynamical matrix, $D_{ij}^{\alpha\beta}$, are given by

$$D_{ij}^{\alpha\beta} = -\frac{1}{2}\left[\frac{F_i^{\alpha}(\{\mathbf{R}\}+d_j^{\beta}) - F_i^{\alpha}(\{\mathbf{R}\}-d_j^{\beta})}{2d_j^{\beta}} + \frac{F_j^{\beta}(\{\mathbf{R}\}+d_i^{\alpha}) - F_j^{\beta}(\{\mathbf{R}\}-d_i^{\alpha})}{2d_i^{\alpha}}\right] \tag{12}$$

where F_j^{α} is the force on atom α in the direction i and $\{\mathbf{R}\}+d_j^{\beta}$ is the atomic configuration where only the atom β is displaced along j from its equilibrium position. The value of displacement was chosen to be 0.03 au (1 au = 0.5292 Å). The equilibrium structure was relaxed to satisfy the maximum forces below 5×10^{-5} Ryd au^{-1}. For this accuracy, the grid spacing h is reduced to 0.4 au as compared to a value of about 0.7 au, typically used for electronic properties. The Chebyshev filtering algorithm is especially well suited for this procedure as the initial diagonalization need not be repeated when the geometry changes are small.

The vibrational mode frequencies and corresponding eigenvectors can be obtained from the dynamical equation:

$$\sum_{\beta,k}\left[\omega^2\delta_{\alpha\beta}\delta_{ik} - \frac{D_{ij}^{\alpha\beta}}{\sqrt{M_\alpha M_\beta}}\right]A_k^{\beta} = 0 \tag{13}$$

where M_α is the mass of an atom labeled by α and the eigenvectors are given by the mode amplitudes, A_k^{β}.

We considered a series of Si nanocrystals: $Si_{29}H_{36}$, $Si_{66}H_{64}$, $Si_{87}H_{76}$ and $Si_{281}H_{172}$. The surface of the nanocrystals were passivated by hydrogen atoms [26] where we avoid any 'one-fold' coordinated Si surface atoms. The interior of the nanocrystal assumes the diamond structure with the relaxed bond length of 2.31 Å.

In figure 6, we illustrate the evolution of the vibrational density of states. The general features appear even in the smallest nanocrystal as the modes are dominated by nearest-neighbor interactions. The modes can be ascribed as follows. The lowest energy modes (below ~200 cm^{-1}) are Si bond bending modes. Si bond stretching modes occur at higher energies (below ~600 cm^{-1}). The dominant peak near 500 cm^{-1} corresponds to the crystalline peak transverse optical (TO) mode. The TO mode is Raman active in crystalline Si and is claimed to be size-dependent [28, 29]. The region above the Si–Si bond stretching modes is related to Si–H dominated vibrations such as librations and scissor motions. This modes are separated from the Si–H stretching modes by a gap from 1000 to 2000 cm^{-1}.

In figure 7, we compare the measured vibrational modes for crystalline silicon [27] to the modes for the largest nanocrystal that we have considered. We ignored the Si–H modes by limiting the comparison to modes below 600 cm^{-1}. The Van Hove singularities in the vibrational density of states have clearly evolved by a nanocrystal containing a few hundred atoms. A similar evolution of the electronic states would not occur until the size of the nanocrystal exceeds several thousand atoms.

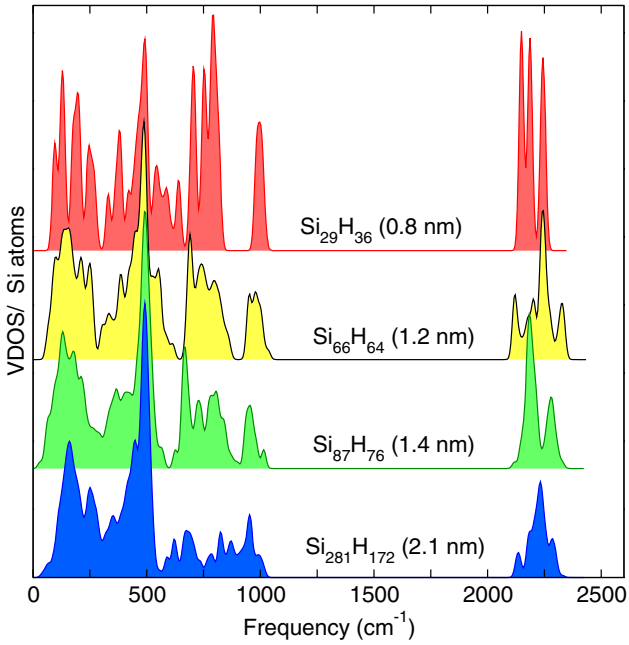

Figure 6. Evolution of vibrational modes in Si nanocrystals. For a better visualization, the intensities of the spectra for each cluster were divided by the number of Si atoms in the corresponding cluster.

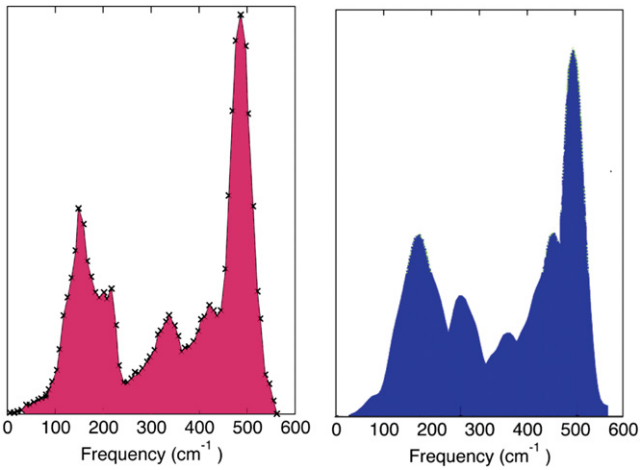

Figure 7. Vibrational modes in bulk silicon from experiment (left) and calculated modes for a nanocrystal ($Si_{281}H_{172}$). The experimental results are from [27].

6. Conclusions

The algorithm presented in this paper replaces the explicit eigenvalue calculations by an approximation of the wanted invariant subspace, obtained with the use of Chebyshev polynomial filters [12]. In our approach, only the initial self-consistent-field iteration requires solving an eigenvalue problem in order to provide a good initial subspace. In the remaining iterations, no iterative eigensolvers are involved. Instead, Chebyshev polynomials are used to refine the subspace. The subspace iteration at each step is easily five to ten times faster than solving a corresponding eigenproblem by the most efficient eigenalgorithms. Moreover, the subspace iteration reaches self-consistency within roughly the same number of steps as an eigensolver-based approach.

We illustrated this algorithm by applying it to hydrogenated silicon nanocrystals for both electronic and vibrational modes. The largest dot we examined contained over 10 000 atoms and was ∼7 nm ($Si_{9041}H_{1860}$) in diameter. We examined the evolution of the electronic properties in these nanocrystals, which we found to assume a bulk-like configuration for dots larger than ∼5 nm. In addition, we obtained scaling relations for the ionization potential, the electron affinity and the quasi-particle gap over the size regime of interest. We found the quasi-particle gap to approach the known bulk limit within density functional theory. We did a similar calculation for vibrational modes, although the size of the nanocrystals is not as large, owing to computational issues, i.e. the need for more accurate forces, and that the vibrational modes converge to the bulk values more rapidly than the electronic states.

Acknowledgments

This work was supported in part by the National Science Foundation under DMR-0551195 and the US Department of Energy under DE-FG02-89ER45391, DE-FG02-03ER25585 and DE-FG02-03ER15491. Calculations were performed at the Texas Advanced Computing Center (TACC), Minnesota Supercomputing Institute (MSI) and National Energy Research Scientific Computing Center (NERSC). Research performed at Oak Ridge National Laboratory was sponsored by the Division of Materials Sciences Engineering BES, US Department of Energy under contract with UT-Battelle, LLC.

References

[1] Alivisatos A P 1996 *Science* **271** 933
Alivisatos A P 1996 *J. Phys. Chem.* **100** 13226
[2] Murray C B, Kagan C R and Bawendi M G 2000 *Ann. Rev. Mater. Sci.* **30** 545
[3] Cullis A G, Canham L T and Calcott P D J 1997 *J. Appl. Phys.* **82** 909
[4] Delerue C, Allan G and Lannoo M 1993 *Phys. Rev.* B **48** 11024
[5] Kohn W and Sham L J 1965 *Phys. Rev.* **140** A1133
[6] Chelikowsky J R 2000 *J. Phys. D: Appl. Phys.* **33** R33
[7] Chelikowsky J R and Cohen M L 1992 *Handbook on Semiconductors* vol 1, ed T S Moss and P T Landsberg, p 59
[8] Kresse G and Furthmüller J 1996 *Phys. Rev.* B **54** 11169
[9] Chelikowsky J R, Troullier N and Saad Y 1994 *Phys. Rev. Lett.* **72** 1240
[10] Torsti T, Eirola T, Enkovaara J, Hakala T, Havu P, Havu V, Höynälänmaa T, Ignatius J, Lyly M, Makkonen I, Rantala T T, Ruokolainen J, Ruotsalainen K, Räsänen E, Saarikoski H and Puska M J 2006 *Phys. Status Solidi* b **243** 1016
[11] Kronik L, Makmal A, Tiago M L, Alemany M M G, Jain M, Huang X, Saad Y and Chelikowsky J R 2006 *Phys. Status Solidi* b **243** 1063
[12] Zhou Y, Saad Y, Tiago M L and Chelikowsky J R 2006 *Phys. Rev.* E **74** 066704
[13] Beck T L 2000 *Rev. Mod. Phys.* **72** 1041
[14] Fornberg B and Sloan D M 1994 *Acta Numer.* **94** 203
[15] Stathopoulos A, Öğüt S, Saad Y, Chelikowsky J R and Kim H 2000 *IEEE Comput. Sci. Eng.* **2** 19
[16] Bekas C, Saad Y, Tiago M L and Chelikowsky J R 2005 *Comput. Phys. Commun.* **171** 175

[17] Lehoucq R B, Sorensen D C and Yang C 1988 *ARPACK Users' Guide: Solution of Large Scale Eigenvalue Problems by Implicitly Restarted Arnoldi Methods* (Philadelphia: SIAM)
[18] Wu K, Canning A, Simon H D and Wang L-W 1999 *J. Comput. Phys.* **154** 156
[19] Foster I 1995 *Designing and Building Parallel Programs* (Reading, MA: Addison-Wesley)
[20] Furukawa S and Miyasato T 1988 *Phys. Rev.* B **38** 5726
[21] Öğüt S, Chelikowsky J R and Louie S G 1997 *Phys. Rev. Lett.* **79** 1770
[22] Sham L J and Schlüter M 1983 *Phys. Rev. Lett.* **51** 1888
Perdew J P and Levy M 1983 *Phys. Rev. Lett.* **51** 1884
[23] Parlinski K, Li Z Q and Kawazoe Y 1997 *Phys. Rev. Lett.* **78** 4063
[24] Alemany M M G, Manish J, Kronik L and Chelikowsky J R 2004 *Phys. Rev.* B **69** 075101
[25] Postnikov A V, Pagès O and Hugel J 2005 *Phys. Rev.* B **71** 115206
[26] Huang X, Lindgren E and Chelikowsky J R 2005 *Phys. Rev.* B **71** 165328
[27] Kamitakahara W A, Soukoulis C M, Shanks H R, Buchenau U and Grest G S 1987 *Phys. Rev.* B **36** 6539
[28] Zhao X-S, Ge Y-R and Zhao X 1998 *J. Mater. Sci.* **33** 4267
[29] Meier C, Lüttjohann S, Kravets V G, Nienhaus H, Lorke A and Wiggers H 2006 *Physica* E **32** 155